Journal of Applied Polymer Science

Synthesis of a branched photosensitive copolymer and its application for negative-type photoresists

Hu Li,[1] Jingcheng Liu,[1] Xiangfei Zheng,[2] Changwei Ji,[2] Qidao Mu,[2] Ren Liu,[1] Xiaoya Liu[1]
[1]Key Laboratory of Food Colloids and Biotechnology (Ministry of Education), School of Chemical and Material Engineering, Jiangnan University, Wuxi 214122, China
[2]Suzhou Rui Hong Electronic Chemicals Company, Limited, Suzhou Jiangsu 215124, China
Correspondence to: X. Liu (E-mail: lxy@jiangnan.edu.cn)

ABSTRACT: Novel branched copolymers, poly(styrene-*alt*-maleic anhydride) (BPSMA), were synthesized through mercapto chain-transfer polymerization with styrene, maleic anhydride (MA), and 4-vinyl benzyl thiol (VBT). Then, the hydroxyl of hydroxyethyl methacrylate was reacted with MA to synthesize branched photosensitive copolymers, *p*-BPSMAs. Fourier transform IR spectroscopy and ^{1}H-NMR indicated that the synthesis was successful. Gel permeation chromatography indicated that the molecular weight decreased with increasing content of VBT. The thermal properties were characterized by thermogravimetric analysis; the results show that the thermal decomposition temperature of the BPSMAs was greatly enhanced. Real-time IR was used to evaluate the UV-curable kinetics of the *p*-BPSMAs; the results show that the *p*-BPSMAs could rapidly photopolymerize under UV irradiation in the presence of photoinitiators. Moreover, the photoresist based on the *p*-BPSMAs exhibited improved photosensitivity when the VBT content increased, and the photoresist with 12 mol % VBT content had a low value of the dose that retained 50% of the original film thickness (10 mJ/cm^2), and a 50-μm resolution could be achieved compared to a linear photoresist. © 2015 Wiley Periodicals, Inc. J. Appl. Polym. Sci. **2016**, *133*, 42838.

KEYWORDS: applications; copolymers; dendrimers; hyperbranched polymers and macrocycles; photopolymerization

Received 13 May 2015; accepted 14 August 2015
DOI: 10.1002/app.42838

INTRODUCTION

Photoresists have been successfully used as pattern materials for photofabrication processes, such as microelectronics manufacturing,[1,2] printed circuit board manufacturing,[3] nanoimprinting,[4,5] and color filter manufacturing.[6] On the basis of the imaging mechanism during development, the photoresist is usually classified as positive or negative type. For negative-type photoresists, exposure renders the resist more insoluble in developer compared to the unexposed area; this leaves the desired circuit patterns on the substrate. The negative photoresist mainly consists of resin, initiator, and solvent; the resin is one of the most important constituents, and its performance directly decides the quality of the image pattern.

Many efforts have focused on linear copolymers or network resins.[7–10] Chang and Yang[11] synthesized a series of methacrylate copolymers used for photoresists; the copolymers were photosensitive toward ultraviolet (UV) exposure, and the resolution capacity reached 10 μm. Lee and Cheng[10] prepared three-component acrylic copolymers used as negative photoresists; the glass-transition temperature (T_g) and viscosity increased as the methacrylic acid content increased. Because the copolymer or network properties play a vital role in photoresists, it is imperative to exploit novel resins with excellent performances used for photoresists.

Recently, hyperbranched polymers have attracted a great deal of attention as dendritic molecules because of some of their interesting properties compared to their linear counterparts; these include good solubility, low viscosity, and high functionality, although many reports on the synthesis and characterization of hyperbranched polymers have been published during the past decades.[12–16] Chatterjee and Ramakrishnan[17] synthesized photodegradable, hyperbranched polyacetal by suitably designing an AB_2 monomer; an HB photoresist was used to create reactive micropatterns. These HB materials often involve iterative synthesis procedures with purification after the completion of each reaction cycle, and they are not very attractive from an industrial point of view.[18] Previously, we reported the one-pot synthesis and characterization of branched P(St-*alt*-MA) via a free-radical polymerization approach;[19,20] this material was used as a dispersant for the preparation of carbon black[21,22] and carbon nanotubes. However, few works are available concerning their applications as photosensitive polymers.[23]

© 2015 Wiley Periodicals, Inc.

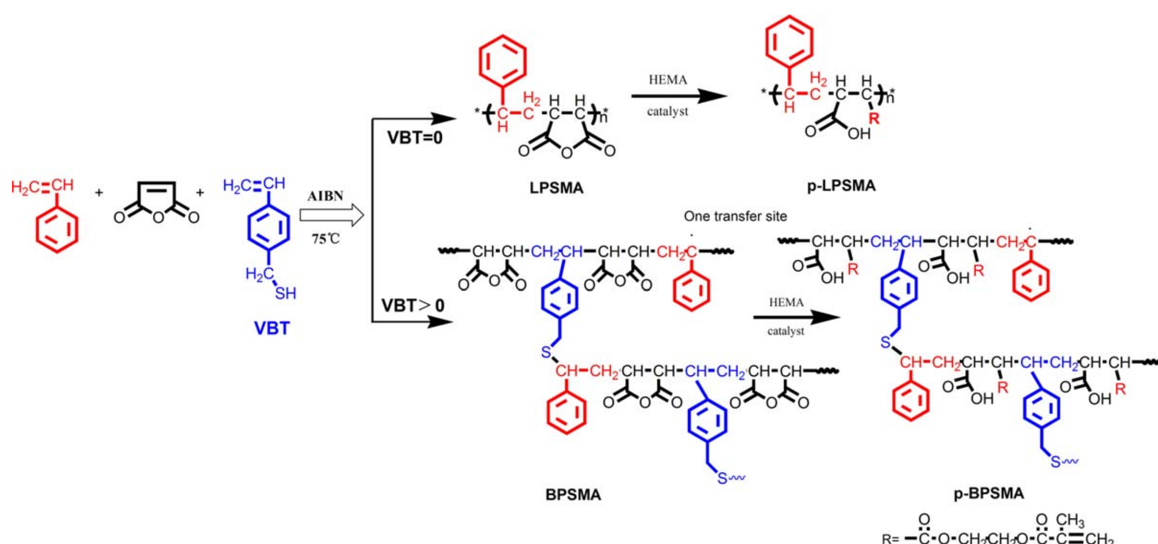

Scheme 1. Polymerization process of the *p*-LPSMA and *p*-BPSMAs. [Color figure can be viewed in the online issue, which is available at wileyonlinelibrary.com.]

In this article, we describe the application of branched P(St-*alt*-MA) as negative photoresist, starting from hydroxyethyl methacrylate (HEMA) grafted into P(St-*alt*-MA), making it a potentially useful candidate for photopatterning material, and characterized by Fourier transform infrared (FTIR) spectroscopy and ^{1}H-NMR. The photopolymerization behaviors were measured by real-time IR analysis, and the photoresist performances in terms of the sensitivity, dissolution rate, kinetics behavior, and pattern resolution were also investigated. A scanning electron microscope was used to observe the morphology and line patterns of photoresists.

EXPERIMENTAL

Materials

Styrene (St; Sinopharm Chemical Reagent Co., Ltd.) was dried by CaH_2 for 24 h and distilled under reduced pressure before use. Maleic anhydride (MA; Aladdin) was recrystallized twice before use. Thiourea and 4-vinyl benzyl chloride were purchased from Aladdin Industry Corp. Ethanol, toluene, 4-methoxyphenol, sodium carbonate anhydrous, tetrahydrofuran, and *n*-hexane were obtained from Sinopharm Chemical Reagent (China). 4-Vinyl benzyl thiol (VBT) was synthesized in our laboratory. Propylene glycol monomethyl ether acetate (PMA) was supplied by Wuxi Meihong Chemical Co. (China). 2-Methyl-4′-(methylthio)-2-morpholinopropiophenone (907) and 2-Isopropylthioxanthone (ITX) as photoinitiators were supplied by Ciba (Switzerland). Trimethylol propanetriacrylate (TMPTA) was obtained from Kuangshun Co. (China). The initiator, azobisisobutyronitrile (AIBN), supplied by Sinopham Chemical Reagent, was purified by recrystallization in ethanol.

Synthesis of the Branched Polymers

The chain-transfer agent VBT was synthesized from 4-vinyl benzyl chloride according to the literature.[21] Then, a series of linear (LPSMA) and branched polymers, poly(styrene-*alt*-maleic anhydride) (BPSMA), was synthesized through chain-transfer polymerization with VBT as a chain-transfer agent. Scheme 1 shows the synthesis of BPSMA and *p*-BPSMA. The LPSMA and *p*-LPSMA were prepared for the purposes of comparison. Amounts of 0.01 mol of St and 0.012 mol of MA, the initiator (AIBN, 1.5 mol % of total monomers), and a desired amount of VBT (3, 6, 9, and 12 mol % of total monomers) were added to a four-necked reactor with 50 mL of toluene and heated to 70°C in oil bath. The solution was mechanically stirred continuously for 24 h in a nitrogen atmosphere; the resulting branched and linear polymers were precipitated from toluene until the sediments were pure, and then, they were dried *in vacuo* at 30°C overnight.

Synthesis of the Photosensitive Polymers

The dried LPSMA and BPSMAs were dissolved in the PMA solvent, and droplets of mixed solution containing a certain amount of graft monomer HEMA, catalyst TPP (TPP/HEMA = 1.5:100 w/w), and inhibitor 4-methoxyphenol (4-methoxyphenol/HEMA = 1.5/100 w/w) were added gradually into the solution within 0.5 h. The reaction was completed until the acid value was constant; then, the product was cooled down to room temperature, and a series of photosensitive linear polymers (*p*-LPSMA) and branched (*p*-BPSMAs) with different contents of VBT were obtained.

The product dissolved in tetrahydrofuran was added to toluene to obtain polymer sediments. This process was repeated three times. The sediments were placed in a vacuum oven and left overnight to obtain purified *p*-LPSMA and *p*-BPSMAs, and then, we identified the chemical structure, molecular weight, and thermal behavior. The properties of a series of copolymers are demonstrated in Table I.

Preparation of the Negative Photoresists

We prepared the negative photoresists by combining the *p*-LPSMA and *p*-BPSMAs, reactive diluent TMPTA, photoinitiator, and solvent at room temperature. The resolution of the negative photoresist was determined by examination of the developed

Table I. Properties of the Photosensitive Branched Copolymers

Sample	VBT (mol %)	n(St):n(MA):n(HEMA)[a] Theoretical feed ratio	Final feed ratio	M_n (g/mol)	Polydispersity index	S content[b]	Yield (%)
p-LPSMA	0	1:1.2:1.2	1:1.25:0.8	15,046	2.84	0	85.7
p-BPSMA-1	3	1:1.2:1.2	1:0.88:0.48	4882	1.23	1.01	80.4
p-BPSMA-2	6	1:1.2:1.2	1:0.95:0.52	4375	1.27	1.21	79.3
p-BPSMA-3	9	1:1.2:1.2	1:0.95:0.55	4104	1.17	2.02	70.4
p-BPSMA-4	12	1:1.2:1.2	1:0.96:0.63	3631	1.21	2.52	69.4

M_n, number-average molecular weight.
[a] The theoretical and final feed ratios were calculated with ^{1}H-NMR.
[b] The S content was measure with an elemental analyzer.

circuit diagram mask under a microscope, and Table II shows the formulation of the photoresist.

Analysis and Characterization

Structure and Property Characterization. FTIR spectroscopy was used to characterize the structures of the polymers. FTIR spectra were acquired on an FTLA2000-104 spectrophotometer in the wavelength range 4500–500 cm^{-1} (ABB Bomem, Canada). ^{1}H-NMR spectra were acquired with a Bruker Avance 300 spectrometer [400 MHz, hexadeuterated dimethyl sulfoxide (d_6-DMSO)]. Scanning electron microscopy (S-4800, Hitachi, Japan) was performed with an electron voltage of 3 kV. Differential scanning calorimetry (DSC) was performed on a DSC822e (Mettler Toledo, Switzerland); the temperature range was from 20 to 140°C with a heating rate of 10°C/min in a nitrogen flow. An appropriate amount of dried sample was sealed in an aluminum pan and placed in the heating chamber together with an empty reference pan. The T_gs of the samples were determined from the thermogram of the second heating cycle. Real-time IR spectroscopy was recorded on a Nicolet 6700 instrument (Thermo Fisher Scientific Co.). The mixture of copolymer and initiator was coated on KBr pellets. The double-bond conversion of the mixture was monitored with near-IR spectroscopy with resolution of 4 cm^{-1} and irradiated with UV radiation by a UV spotlight source (OmniCure series 1000, EXFO Co., Canada) at room temperature. Vario EL III elemental analyzer (Elementar Co., Germany) was used to analyze the S content in the samples. Thermogravimetric analysis (TGA; Mettler Toledo, Switzerland) was used to measure the thermal decomposition temperature, and the samples (5–10 mg) were heated from 25 to 600°C at a heating rate of 20°C/min in a nitrogen flow.

Table II. Formulation of the Photoresist

Ingredient	%
p-BPSMA or p-LPSMA	65
Photoinitiator (907 and ITX)	5
Monomer (TMPTA)	15
Casting solvent (PMA)	15

Dissolution Behavior Analysis. When p-LBPSMAs with different VBT contents and p-LPSMA were spin-coated on copper substrates, the coated samples were prebaked in an oven at 75°C for 30 min to remove the solvent. The samples were cooled down to room temperature in air, weighed, and immersed in developer (1wt % Na_2CO_3) for a designated time. Then, the developed photoresists were postbaked (at 75°C for 30 min) to a constant weight. The dissolution behavior, characterized by the elution rate of the photoresist, was calculated with the following equation:

$$\text{Dissolution rate} = \frac{W_2 - W_3}{W_2 - W_1} \times 100\%$$

where W_1 is the copper substrate weight, W_2 is the copper substrate weight after prebaking, and W_3 is the copper substrate weight after postbaking.

Photosensitivity Analysis. The parameters of photosensitivity were determined by a UV energy meter (UVint140) and were defined as the dose that retained 50% of the original film thickness (δ_o) after development ($D_n^{0.5}$). The exposure dose was 0–100 mJ/cm^2, and the residual rate of film thickness (∂) was calculated as follows:

$$\partial = \frac{\delta}{\delta_o}$$

where δ is the film thickness after development.

RESULTS AND DISCUSSION

FTIR Analysis

Figure 1 shows the FTIR spectra of BPSMA and p-BPSMA (VBT content = 12%; the structure is shown in Scheme 1). In the BPSMA spectra, 1858 and 1778 cm^{-1} were due to the symmetric and antisymmetric stretching vibration peaks of C═O in MA. The absence of peaks at 1080 and 702 cm^{-1} represented the out-plane and in-plane bend vibrations of benzene. There was no thiol characteristic peak at 2550 cm^{-1}, and the C═C peak was not observed in the spectra of BPSMA; this indicated that the polymerization was complete. Compared to the p-BPSMA spectra, the peak at 1636 cm^{-1} was due to the stretching vibrations of C═C. Additionally, the absorption peak of the carboxyl group appeared at 3500 cm^{-1}; this indicated that

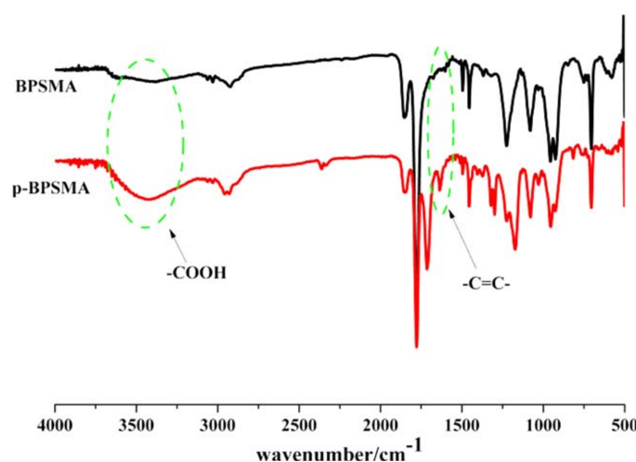

Figure 1. FTIR spectra of BPSMA and *p*-BPSMA with 12% VBT. [Color figure can be viewed in the online issue, which is available at wileyonlinelibrary.com.]

HEMA reacted with MA. Namely, HEMA was grafted to BPSMA, and this introduced the double bond successfully.

^{1}H-NMR Analysis

Figure 2 shows the ^{1}H-NMR spectra of BPSMA and *p*-BPSMA (VBT content = 12%). The peaks at 5.6 and 6.0 (H13) were obvious, and this confirmed the existence of HEMA in the *p*-BPSMA molecular structure. Moreover, the signal peak at 12.2 ppm originated from the —COOH group (H15). Additionally, the signals at 1.7 and 0.9 ppm were assigned to protons (H2 and H6) in the main chain of BPSMA. The previous analysis confirmed that the synthesis of the UV-curable *p*-BPSMA was successful, and this was in accordance with the FTIR results.

Photopolymerization Kinetics of the *p*-BPSMAs and *p*-LPSMA

The most important parameters characterizing the photopolymerization behavior of the UV-cured film were the rate at the

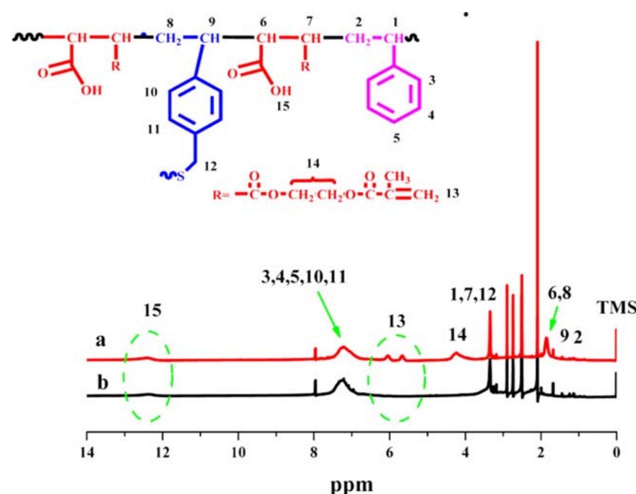

Figure 2. ^{1}H-NMR spectra of BPSMA and *p*-BPSMA in *d*-DMSO. [Color figure can be viewed in the online issue, which is available at wileyonlinelibrary.com.]

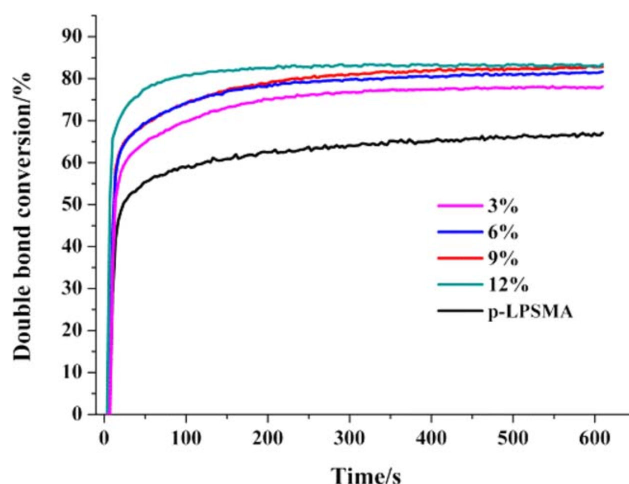

Figure 3. Real-time IR spectrum with different VBT contents of *p*-BPSMAs (1636-cm^{-1} double-bond conversion). [Color figure can be viewed in the online issue, which is available at wileyonlinelibrary.com.]

peak maximum (R_p^{max}) and the final degree of double-bond conversion after a given irradiation time.[24,25] The UV-curing kinetics of the *p*-LPSMA and *p*-BPSMAs with different VBT contents are shown in Figure 3. The photopolymerization rate of each sample showed a steep increase at the start of reaction, reaching R_p^{max}. Such results were explained on the basis of the chain-transfer reaction involving the hydroxyl groups present on the surface of the branched polymer. Because of the chain-transfer mechanism, the network structure became more flexible, and the mobility of the reactive species increased. This reduced the viscosity,[26] so the curing rate of double-bond conversion increased. As for *p*-LPSMA, a dramatic increase in the polymerization rate was observed at low double-bond conversion; this was because the decreased mobility that occurred as the viscosity increased could have increased the film thickness under the same spin speed and reduced the penetration of UV radiation into the sample. This caused a reduction in the termination rate constant.[27,28] In general, the VBT caused an increase in R_p^{max}, which was associated with the low diffusivity of the polymer matrix, and this fact was more noticeable for *p*-BPSMA with a high VBT content.

Thermal Decomposition Analysis (TGA) of *p*-BPSMA and *p*-LPSMA

The thermal properties of copolymers play a major role in determining their applications. Figure 4 shows the TGA curves of *p*-BPSMAs with different VBT contents and *p*-LPSMA. As indicated in the figure, the addition of VBT raised the thermal temperature compared to that of *p*-LPSMA; when a 10% weight loss was selected as the point of comparison, the decomposition temperatures of the p-LPSMA, *p*-BPSMA-1, *p*-BPSMA-2, *p*-BPSMA-3, and *p*-BPSMA-4 samples were determined to be 197.2, 212.5, 226.5, 234.8, and 250.3°C, respectively. However, all of the TGA curves of the copolymers showed complicated and mainly two-stage decompositions. The first stage of weight loss, occurring from 180 to 250°C, was attributed to the degradation of the terminal groups grafted by HEMA.[29] The second

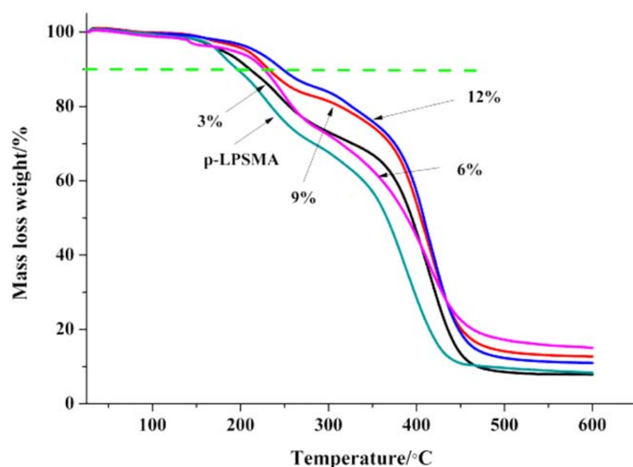

Figure 4. TGA curves of the *p*-LPSMA and *p*-BPSMAs with different VBT contents. [Color figure can be viewed in the online issue, which is available at wileyonlinelibrary.com.]

stage, appearing from 250 to 300°C, was ascribed to polymer chain degradation, a complex process including double-bond thermal crosslinks, and the weight loss in this stage reached a maximum.[30,31]

DSC Analysis

The DSC curves of the *p*-BPSMA and *p*-LPSMA samples are enumerated in Figure 5. T_g was overly affected by the polymer chain mobility; for branched polymers with low viscosity, T_g decreased as the VBT content increases. This was probably because the large number of end groups improved the polymer chain free volume and mobility. Then, T_g decreased.[32–34] As for *p*-LPSMA, its T_g was higher than that of *p*-BPSMAs because of the high viscosity and rigid polymer chain.

Dissolution Behavior Analysis

To investigate the lithographic performance of the exposed and unexposed areas, the effects of different VBT contents of the *p*-BPSMAs and *p*-LPSMA on the dissolution rate were first studied through the measurement of the film weight after development.[35] It was proven that the branching degree of BPSMA increased with increasing amount of VBT. Hence, the dissolution rate of the *p*-BPSMAs improved notably compared to *p*-LPSMA, with an increased amount of —COOH produced in end group of the *p*-BPSMAs. A pictorial representation of the dissolution rate for the *p*-LPSMA and *p*-BPSMAs with different VBT contents is summarized in Figure 6.

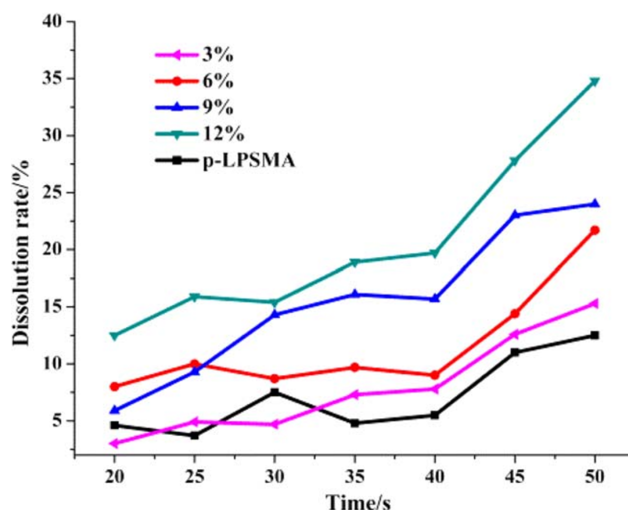

Figure 6. Curves of the dissolution rate with different VBT contents. [Color figure can be viewed in the online issue, which is available at wileyonlinelibrary.com.]

Photosensitivity Analysis

The photosensitivity of the photoresists was measured by the parameter $D_n^{0.5}$. Figure 7 represents the curves of all of the photoresists for exposure doses ranging from 0 to 120 mJ/cm^2. $D_n^{0.5}$ for the *p*-LPSMA was 58.3 mJ/cm^2, whereas the $D_n^{0.5}$ values of the *p*-BPSMAs of the samples with 3, 6, 9, and 12% VBT contents were 55.6, 50.8, 34.8, and 29.9 mJ/cm^2, respectively. Obviously, $D_n^{0.5}$ decreased with increasing VBT. This indicated a better photosensitivity with the addition of VBT. This could

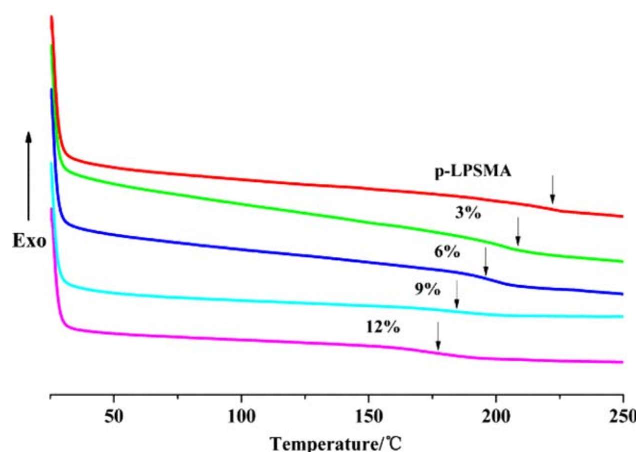

Figure 5. DSC thermograms of the *p*-LPSMA and *p*-BPSMAs with different VBT contents. [Color figure can be viewed in the online issue, which is available at wileyonlinelibrary.com.]

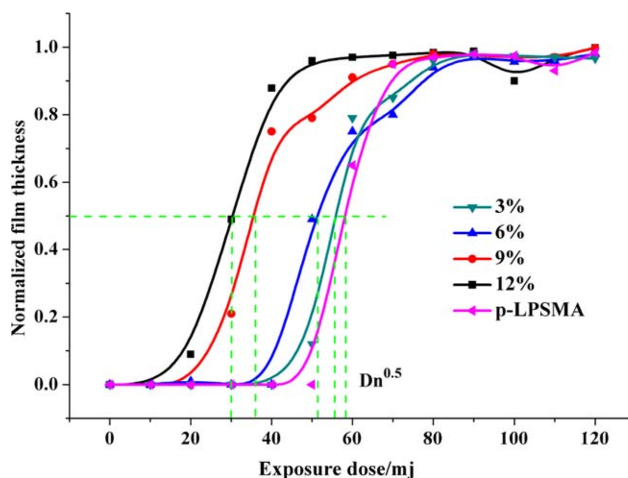

Figure 7. Characteristic curves of the *p*-BPSMAs and *p*-LPSMA. [Color figure can be viewed in the online issue, which is available at wileyonlinelibrary.com.]

Table III. Properties of the Photoresists *p*-LPSMA and *p*-BPSMAs with Different VBT Contents

Polymer	Exposure energy (mJ/cm^2)		γ	Acid value (mg/g)	Graft ratio (%)[a]
	E_0	E_t			
p-LPSMA	50	90	3.92	43.64	76.26
p-BPSMA-1	40	90	2.84	45.12	65.35
p-BPSMA-2	40	80	3.22	47.97	63.99
p-BPSMA-3	20	70	1.84	56.05	41.08
p-BPSMA-4	10	50	1.43	56.99	38.42

[a] The graft ratio was calculated with the acid value.

be explained by the fact that an increased amount of VBT could have enriched the double bond in the end group of the *p*-BPSMAs. This resulted in high-concentration crosslinking and brought about a great improvement in the photosensitivity for the *p*-BPSMAs.

Because the sensitive function group underwent crosslinking for negative photoresists, the film thickness of the unexposed resist film remaining after development was plotted as a function of the exposure dose (mJ/cm^2 for UV irradiation); this reflected the critical gel exposure energy (E_0) and saturated exposure energy (E_t). Then, the contrast (γ) was calculated according to the following equation:

$$\gamma = 1/\lg(E_t/E_0)$$

where E_0 represents the photosensitivity.[36] With the use of 1 wt % Na_2CO_3 as the developer, the characteristic exposure parameters are summarized in Table III. The acid value and composition of the resist matrix greatly affected E_0 and γ; γ increased as the resin acid value decreased.

Resolution of the Photoresists

The photoresist solutions were prepared as described in the Experimental section. It was important to determine the degree of resolution that the photoresist achieved to satisfy the industrial standard.[37] The scanning electron microscopy images of the negative photoresists formed by the *p*-LPSMA and *p*-BPSMAs with 3, 6, 9, and 12% VBT matrix resin contents are shown in Figure 8 under a UV irradiation exposure energy dose of 75 mJ/cm^2 in contact mode with a mask. The exposure time was 5 s because the develop time and —COOH were shown to affect the quality of the patterns in the photoresists. Appropriate —COOH and development time presented a fine linear pattern. For the *p*-BPSMAs, as shown in Figure 8(A–D), because of the large amount of —COOH in the end group of *p*-BPSMA, the develop time was less than 5 s, and we obtained clear lines with a 50-μm resolution. This resolution was attributed to the high degree of branching of the *p*-BPSMAs with low chain entanglement. On the contrary, the *p*-LPSMA needed more than 10 s to develop. It was overdeveloped because of the high viscosity and

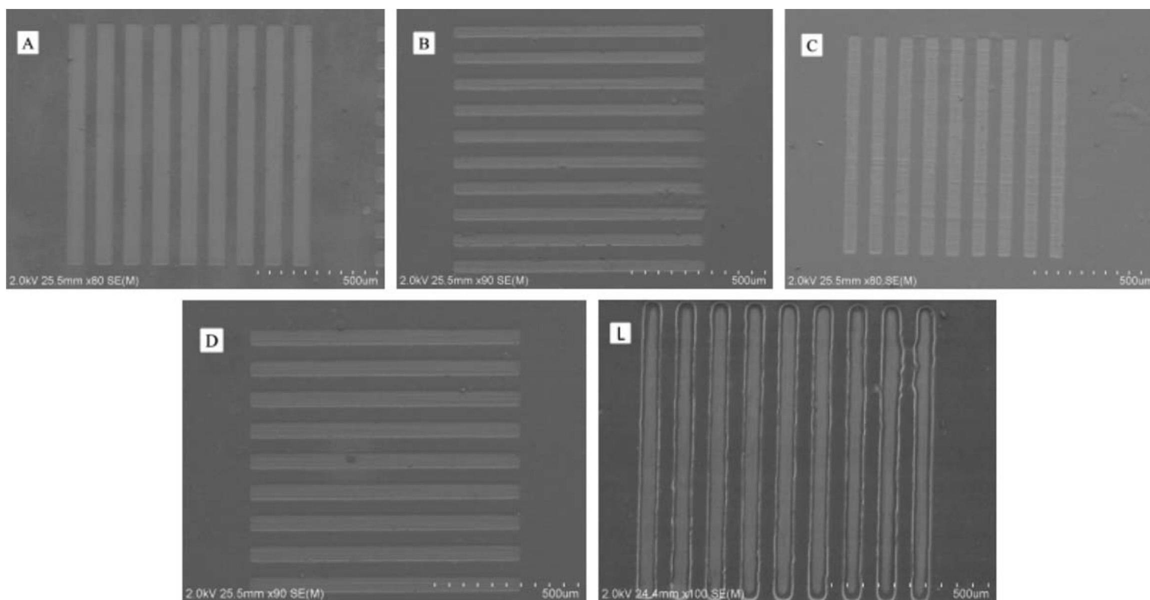

Figure 8. Scanning electron microscopy images of the lithographic pattern for photosensitive *p*-BPSMAs and *p*-LPSMA: (A) 3% VBT, (B) 6% VBT, (C) 9% VBT, (D) 12% VBT, and (L) *p*-LPSMA.

molecular chain mobility; this resulted in a blurred pattern, as shown in Figure 8(L).

CONCLUSIONS

A novel branched copolymer, BPSMA, was synthesized, and HEMA was reacted with MA to synthesize a UV-curable photosensitive. Thus, a series of UV-cured photoresists were prepared. The molecular weights and T_g values decreased with the addition of VBT. $D_n^{0.5}$ was also greatly enhanced with the addition of a chain-transfer agent because of a high concentration of double bonds in the terminal group. Moreover, the thermal and dissolution rates and resolution were also enhanced, and the resolution of the photoresist was 50 μm.

ACKNOWLEDGMENTS

This work was supported by the Jiangsu Postgraduate Scientific Research and Innovation Plan Project (contract grant number KYLX_1127) and the National Science and Technology Major Project of China (contract grant number 2010ZX02304).

REFERENCES

1. Chae, K. H.; Sun, G. J.; Kang, J. K. *J. Appl. Polym. Sci.* **2002**, *86*, 1172.
2. Weibel, G. L.; Ober, C. K. *Microelectron. Eng.* **2003**, *65*, 145.
3. Kerdlapee, P.; Tuantranont, A. *Microsyst. Technol.* **2014**, *20*, 127.
4. Lee, H.; Choi, K. *Microelectron. Eng.* **2006**, *83*, 323.
5. Yoo, S. H.; Jeong, H. *J. Korean Phys. Soc.* **2013**, *63*, 1740.
6. Lee, C. K.; Feng, H. H. *Adv. Polym. Technol.* **2012**, *31*, 163.
7. Jian, H. C.; Yang, H. *J. Polym. Res.* **2013**, *20*, 115.
8. Huang, H. Y.; Chen, H. *J. Thermoplast. Compos.* **2011**, *24*, 51.
9. Huang, H. Y. *Mol. Cryst. Liq. Cryst.* **2011**, *548*, 3.
10. Lee, C. K. *J. Appl. Polym. Sci.* **2008**, *109*, 467.
11. Chang, S.; Yang, J. H. *J. Polym. Res.* **2013**, *20*, 115.
12. Chochos, C. L.; Ismailova, E.; Hadziioannou, G. *Adv. Mater.* **2009**, *21*, 1121.
13. Thompson, D. S. *Macromolecules* **2000**, *33*, 6412.
14. Yamanaka, K.; Kakimoto, M. *Macromolecules* **2001**, *34*, 3910.
15. Ankur, S.; Kulshrestha, R. A. *Biomacromolecules* **2007**, *8*, 1794.
16. Kim, Y. H. *J. Polym. Sci. Part A: Polym. Chem.* **1998**, *36*, 1685.
17. Chatterjee, S.; Ramakrishnan, S. *Chem. Commun.* **2013**, *49*, 11041.
18. Voit, B. I.; Lederer, A. *Chem. Rev.* **2009**, *109*, 5924.
19. Liu, H. V.; Liu, X. Y. *Polym. Bull.* **2013**, *70*, 1795.
20. Liu, J. C.; Liu, X. Y. *Prog. Org. Coat.* **2013**, *76*, 1251.
21. Xu, Y. Y.; Liu, X. Y. *Prog. Org. Coat.* **2012**, *75*, 537.
22. Fu, S. H.; Xu, C. H. *Ind. Eng. Chem. Res.* **2014**, *53*, 10007.
23. Bratton, D.; Ober, C. K. *Polym. Adv. Technol.* **2006**, *17*, 94.
24. Li, G.; Sun, F. *Ind. Eng. Chem. Res.* **2013**, *52*, 2220.
25. Sun, F.; Nie, J. *Prog. Org. Coat.* **2009**, *66*, 412.
26. Corcione, C. E.; Malucelli, G. *Polym. Test.* **2009**, *28*, 157.
27. Larraza, I.; Peinado, C.; Corrales, T. *J. Photochem. Photobiol. A* **2011**, *224*, 46.
28. Foix, D.; Ramis, X.; Sangermano, M. *Polymer* **2011**, *52*, 3269.
29. Han, W. S.; Lin, B. P. *J. Appl. Polym. Sci.* **2013**, *128*, 4261.
30. Subramanian, K.; Vijayakumar, V. *Saudi Pharm. J.* **2012**, *20*, 263.
31. Rani, G. U.; Mishra, S.; Pathakb, G.; Jhaa, U.; Sen, G. *Int. J. Biol. Macromol.* **2013**, *61*, 276.
32. Tasic, S.; Bozic, B.; Dunjic, B. *Prog. Org. Coat.* **2004**, *51*, 321.
33. Huang, Z. G.; Shi, W. F. *Eur. Polym. J.* **2007**, *43*, 1302.
34. Wooley, K. L.; Hawker, C. J.; Pochan, J. M. *Macromolecules* **1993**, *26*, 1514.
35. Ueda, M.; Nakayama, T. *Macromolecules* **1996**, *29*, 6427.
36. Feng, Z. C.; Liu, M. *J. Appl. Polym. Sci.* **2004**, *92*, 1259.
37. Liu, J. H.; Shi, C. H. *J. Appl. Polym. Sci.* **2001**, *81*, 1014.